Specific inhibition of herpes simplex virus DNA polymerase by helical peptides corresponding to the subunit interface

Proc. Natl. Acad. Sci. USA
Vol. 92, pp. 1456–1460, February 1995
Biochemistry

Specific inhibition of herpes simplex virus DNA polymerase by helical peptides corresponding to the subunit interface

(circular dichroism/analytical ultracentrifugation/processivity/rational drug design)

PAUL DIGARD*†, KEVIN P. WILLIAMS‡§, PRESTON HENSLEY¶, IAN S. BROOKS¶, CHARLES E. DAHL*, AND DONALD M. COEN*‖

*Department of Biological Chemistry and Molecular Pharmacology, Harvard Medical School, Boston, MA 02115; ‡Research Division, Joslin Diabetes Center, Boston, MA 02215; and ¶Department of Macromolecular Sciences, SmithKline Beecham Pharmaceuticals, King of Prussia, PA 19406

Communicated by Steven L. McKnight, Tularik, South San Francisco, CA, November 22, 1994

ABSTRACT **The herpes simplex virus DNA polymerase consists of two subunits—a catalytic subunit and an accessory subunit, UL42, that increases processivity. Mutations affecting the extreme C terminus of the catalytic subunit specifically disrupt subunit interactions and ablate virus replication, suggesting that new antiviral drugs could be rationally designed to interfere with polymerase heterodimerization. To aid design, we performed circular dichroism (CD) spectroscopy and analytical ultracentrifugation studies, which revealed that a 36-residue peptide corresponding to the C terminus of the catalytic subunit folds into a monomeric structure with partial α-helical character. CD studies of shorter peptides were consistent with a model where two separate regions of α-helix interact to form a hairpin-like structure. The 36-residue peptide and a shorter peptide corresponding to the C-terminal 18 residues blocked UL42-dependent long-chain DNA synthesis at concentrations that had no effect on synthesis by the catalytic subunit alone or by calf thymus DNA polymerase δ and its processivity factor. These peptides, therefore, represent a class of specific inhibitors of herpes simplex virus DNA polymerase that act by blocking accessory-subunit-dependent synthesis. These peptides or their structures may form the basis for the synthesis of clinically effective drugs.**

Herpes simplex virus (HSV) is a major human pathogen, especially in immunocompromised patients such as those with AIDS. Treatment has relied mainly on the drug acyclovir, whose ultimate target is the virus-encoded DNA polymerase (1). However, antiviral resistance is becoming a problem of increasing clinical significance (2, 3), indicating the need for alternative anti-HSV drugs. The HSV DNA polymerase still remains an attractive drug target, as it is absolutely essential for virus replication (1). Structurally, the enzyme consists of a catalytic subunit (Pol) and a smaller subunit, UL42, that is not necessary for polymerase activity *per se* but increases the processivity of the enzyme (4, 5). Mutations that specifically disrupt subunit interactions ablate virus replication, indicating that these interactions are necessary for virus replication (6, 7). This suggested the attractive possibility of rationally developing a class of polymerase inhibitors designed to interfere with dimerization.

Residues crucial for the Pol–UL42 interaction and viral replication lie at the extreme C terminus of Pol (6, 8, 9). Two potential routes to antiviral drugs based on these residues are (*i*) rational design starting from the structure of this region and (*ii*) the development of peptidomimetic analogues of this region, which could be aided by structural information. Toward these ends, we have conducted biophysical studies of peptides corresponding to the extreme C terminus of Pol. Our results suggest that this region forms a discrete structure, which may be amenable to high-resolution structural analysis. Further, we have shown that certain such peptides specifically block the functional consequences of UL42 binding and prevent processive DNA synthesis, indicating the potential for peptidomimetic development.

The publication costs of this article were defrayed in part by page charge payment. This article must therefore be hereby marked "*advertisement*" in accordance with 18 U.S.C. §1734 solely to indicate this fact.

MATERIALS AND METHODS

Materials. Peptides A and E were synthesized by a solid-phase procedure using fluorenylmethoxycarbonyl chemistry on a Milligen/Biosearch 9600 synthesizer. The peptides were deblocked and cleaved from the resin by trifluoroacetic acid/thioanisole/ethanedithiol/anisole (9:0.5:0.3:0.2, vol/vol) to minimize oxidation of methionine and then precipitated and washed with diethyl ether to remove impurities generated during cleavage. Peptides C, D, and F were generously provided by Bio-Méga/Boehringer Ingelheim. Peptide B and certain lots of peptide E were purchased from Chiron. All peptides were purified by HPLC and lyophilized for storage. Working stocks were dissolved in dimethyl sulfoxide. Peptide identities and concentrations were confirmed by amino acid analysis carried out at the Brigham and Womens Hospital Biopolymer Laboratory.

HSV Pol and UL42 were purified from insect cells infected with the appropriate recombinant baculoviruses (6) and kindly provided by Klaus Weisshart (D.M.C.'s laboratory). Partially purified calf thymus DNA polymerase δ and proliferating-cell nuclear antigen (PCNA) were generously supplied by Bruce Stillman (Cold Spring Harbor Laboratory).

CD Spectroscopy. Lyophilized peptides were resuspended in 10 mM KF and adjusted to pH 8 with KOH. Unless otherwise specified, peptide concentrations were ≈100 μM, except for peptide A, which was 40 μM. All spectra were recorded with an Aviv 62DS spectropolarimeter at 0°C. Wavelength scans were recorded at 1-nm intervals (10-sec averaging time), and at least three scans were averaged.

Analytical Ultracentrifugation. Equilibrium sedimentation experiments on peptide A were performed with a Beckman XL-A analytical ultracentrifuge using double-sector cells with charcoal-filled Epon centerpieces and sapphire windows. Experiments were performed at 4°C and 25°C in 20 mM Hepes/50 mM phosphate, pH 8.0, in H_2O or ^2H_2O with an initial peptide concentration of 30 μM. The distribution of the peptide at various radii was assayed by absorbance at 230 nm. Data were analyzed by nonlinear least-squares methods under the control of a modified version of IGOR-PRO (WaveMetrics,

Abbreviations: HSV, herpes simplex virus; Pol, HSV DNA polymerase catalytic subunit; PCNA, proliferating-cell nuclear antigen.

†Present address: Division of Virology, Department of Pathology, University of Cambridge, Cambridge CB2 1QP, United Kingdom.
§Present address: Bioscience Research, PerSeptive Biosystems, Inc., Cambridge, MA 02139.
‖To whom reprint requests should be addressed.

Lake Oswego, OR) running on a Macintosh computer. Data sets were collected at 18–24 hr, at rotor speeds of 50,000 and 60,000 rpm. Equilibrium was established by determining that scans taken 4 hr apart were superimposible. To determine whether the peptide behaved as a monomer or higher-order assembly, an equation describing the macromolecular distribution at sedimentation equilibrium for monodisperse systems (single ideal species) was employed (10):

$$c_r = c_0 \exp[M(1 - \bar{v}\rho)\omega^2(r^2 - r_0^2)/2RT] + \text{base}, \quad [1]$$

where c_r and c_0 are the total concentrations of species at a radial position, r, and at the meniscus (a reference position). M and $\bar{v}$ are the molecular weight and partial specific volume of the macromolecule, ρ is the solvent density, ω is the angular velocity, r_0 is the reference radial position, R is the universal gas constant, T is the absolute temperature, and base is a baseline term corresponding to optical density from a nonsedimenting material. Because the determination of $\bar{v}$ for peptide A by various predictive methods based on amino acid composition gave very different answers, molecular mass and $\bar{v}$ were measured simultaneously by the method of Edelstein and Schachman (11) as extended by Eisenstein *et al.* (12), using solvents of different densities (H_2O and ^2H_2O). The parameters c_0, M, and base were determined by nonlinear least-squares methods (13, 14). Data were analyzed in terms of assembly models by fitting the data to sums of exponentials, one for each additional species (14).

Polymerase Assays. Reaction mixtures (25 μl) containing 50 mM Tris·HCl (pH 7.6), 100 mM $(NH_4)_2SO_4$, 3 mM $MgCl_2$, 0.1 mM EDTA, 1 mM dithiothreitol, 4% (vol/vol) glycerol, 1 μg of bovine serum albumin, 10% (vol/vol) dimethyl sulfoxide, 50 μM dTTP, 0.25 μg of a poly(dA)·oligo(dT) template (15, 16), 25 fmol of HSV Pol, either no or 50 fmol of UL42, and the indicated concentrations of a given peptide were incubated at 37°C for 30 min. In the experiment shown here, peptide A was preincubated on ice for 15 min with UL42 in the reaction mixture, and Pol was added last, whereas in other experiments, there was no preincubation and UL42 was added last. Preincubation increased the potency of peptide A about 10-fold but had little or no effect on the potencies of other peptides (data not shown). DNA synthesis was terminated by the addition of 3 volumes of 20 mM EDTA/1% SDS containing salmon sperm DNA (10 μg/ml), and the samples were ethanol precipitated before electrophoresis in alkaline agarose gels. Newly synthesised DNA was detected by autoradiography and quantified by densitometry. For reactions containing Pol δ, $(NH_4)_2SO_4$ was omitted from the reaction buffer, and 0.5 μl of Pol δ and 250 ng of PCNA were added in place of HSV Pol and UL42, respectively.

RESULTS

A Peptide Corresponding to the C Terminus of Pol Has α-Helical Character. Previous studies indicated that UL42 binds to the C terminus of Pol (17) and that within this region, residues downstream of aa 1195 are crucial for interaction with UL42 (6, 8, 9). Reasoning that proline residues at positions 1198 and 1199 (Fig. 1) might denote a turn between units of secondary structure, we synthesized a peptide corresponding to the last 36 residues (aa 1200–1235) of Pol (Fig. 1, peptide A). A Robson–Garnier secondary-structure prediction algorithm of this portion of Pol had predicted two regions of α-helical structure interrupted by a poorly predicted region centered on four closely spaced glycine residues (residues 1210–1217) for this region of Pol (Fig. 1), raising the possibility of a hairpin-like helix–loop–helix structure (6). Consistent with this prediction, the CD spectrum of peptide A in aqueous solution (Fig. 2) exhibited double minima at 222 and ≈205 nm and a maximum at 192 nm characteristic of α-helices (19). The

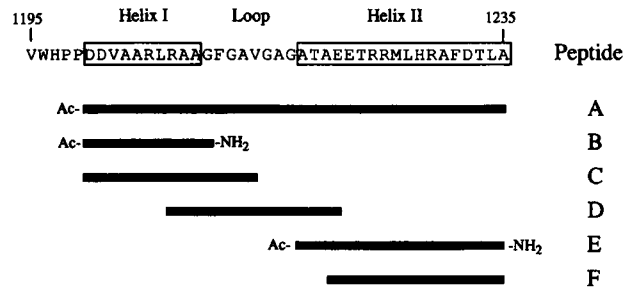

FIG. 1. Peptides corresponding to the C terminus of HSV-1 strain KOS Pol. Residues 1195–1235 (18) (single-letter code) of Pol are shown, with regions of predicted helix boxed. Peptides used in this study are indicated by the bars, with acetylated (Ac-) and amidated (-NH_2) termini shown where appropriate.

intensity of the minimum at 222 nm indicated a helical content of ≈22% (20). Even at 37°C, the value at 222 nm reflected 10–15% helicity (data not shown).

The C-Terminal Peptide Behaves as a Monomer. The degree of helicity of peptide A did not vary substantially over the concentration range 10–50 μM (data not shown) suggesting that the peptide was monomeric in solution, but its limited solubility in UV-transparent buffers precluded analysis over a wider range of concentrations. Therefore we examined peptide A by equilibrium analytical centrifugation to permit analysis of molecular mass over a concentration range of 0.5–100 μM. The analysis was performed in both H_2O and ^2H_2O to permit simultaneous determination of the partial specific volume (11, 12). The distribution of peptide (monitored at 230 nm) with radius (Fig. 3*C*) fit closely, independent of the solvent, to that predicted for a single species, as shown by the small residuals obtained (Fig. 3*A* and *B*). Molecular mass at all concentrations was determined as 3387 ± 334 Da and partial specific volume as 0.715 ± 0.024 ml/g. The mass determined is close to that predicted from the peptide sequence (3727 Da), with no evidence for a dimer or higher-order structure. Similar results were obtained from measurements in H_2O at multiple rotor speeds and temperatures (data not shown). In all cases, analyses of the peptide distribution gave no evidence of species larger than the monomer. Therefore, peptide A is monomeric at concentrations where it exhibits α-helical character.

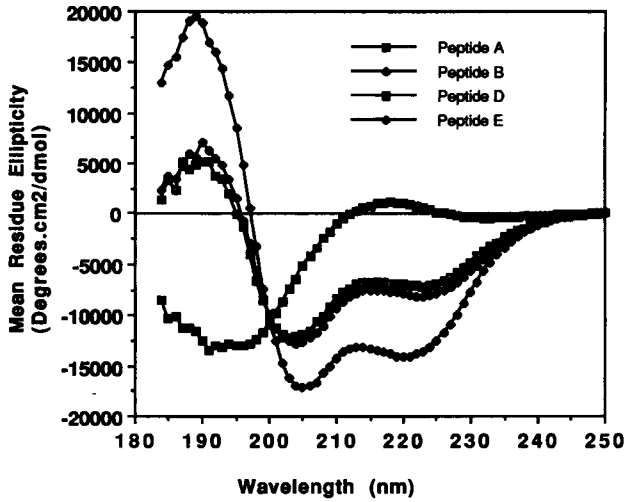

FIG. 2. Analysis of peptide structure. CD spectra of peptides A, B, D, and E. Double minima at 222 and ≈205 nm and a maximum at 192 nm are characteristic spectra of α-helices, while a weak maximum at 215 nm and an intense minimum at 195 nm are characteristic of random coil (19). The mean residue ellipticities indicate helical contents of 22%, 42%, 0%, and 25% (20) for peptides A, B, D, and E, respectively, at 100 μM.

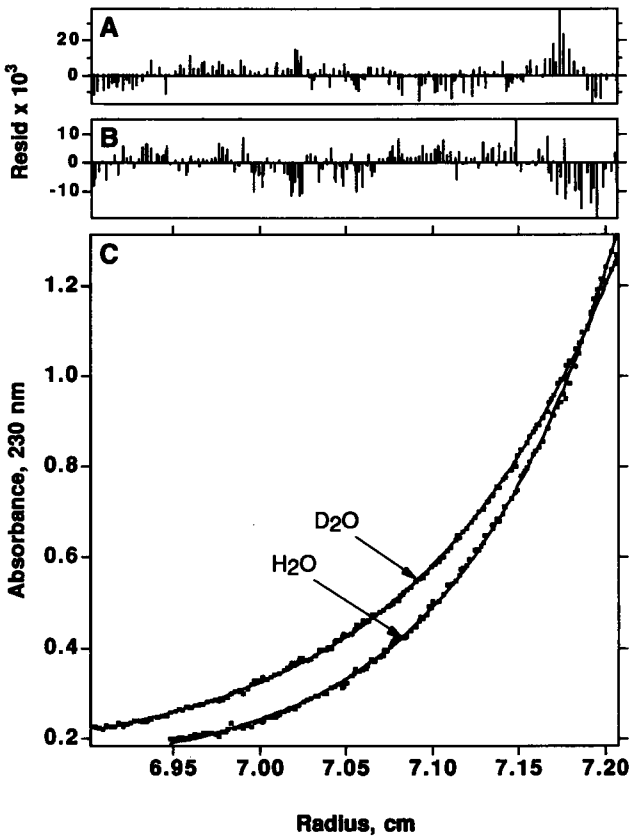

FIG. 3. Equilibrium sedimentation data for peptide A in H_2O and ^2H_2O (D_2O). (*A* and *B*) Residuals (theoretical for a single ideal species − observed values at each data point) for the H_2O and D_2O data, respectively. (*C*) Primary equilibrium sedimentation data.

Helicity of Shorter Peptides. One way that peptide A could fold into a monomer with α-helical character would be for the separate regions of predicted helix to interact. We therefore synthesized peptides corresponding to separate regions of peptide A (Fig. 1). CD spectra for peptides B and E, which correspond to predicted helices I and II (Fig. 1), showed substantial levels of α-helix at concentrations of 100 μM in aqueous solution (Fig. 2). The intensities of the minima at 222 nm indicated helical contents of ≈42% and ≈25% for peptides B and E, respectively. In contrast, peptide D, corresponding to the glycine-rich region (Fig. 1), displayed a spectrum characteristic of a random coil, with a weak maximum at 218 nm and an intense minimum at 195 nm (Fig. 2). We next tested whether the helicities of peptides B and E were concentration dependent. The mean residue ellipticities at 222 nm decreased substantially with lower peptide concentrations, suggesting that helicity depended on the formation of dimers or other higher-order structures (data not shown). This was consistent with the predicted amphipathic nature of the helices (6) but was in contrast to the behavior of peptide A.

The 36-Residue Peptide Inhibits UL42-Mediated Long-Chain DNA Synthesis. We hypothesized that peptides corresponding to the C terminus of Pol could inhibit the Pol–UL42 interaction. We therefore tested the ability of peptide A to inhibit UL42-dependent long-chain DNA synthesis, using a modification of a previously reported assay (15, 16). In this assay, a ^{32}P-labeled primer on a homopolymeric template was extended only a short distance by Pol alone (Fig. 4*A*, lane 3) but was extended considerably further in the presence of UL42 (lane 4; for control reactions without Pol, see lanes 1 and 2). Increased chain length in the presence of UL42 reflects an increase in the processivity of the enzyme (4, 5, 16) and

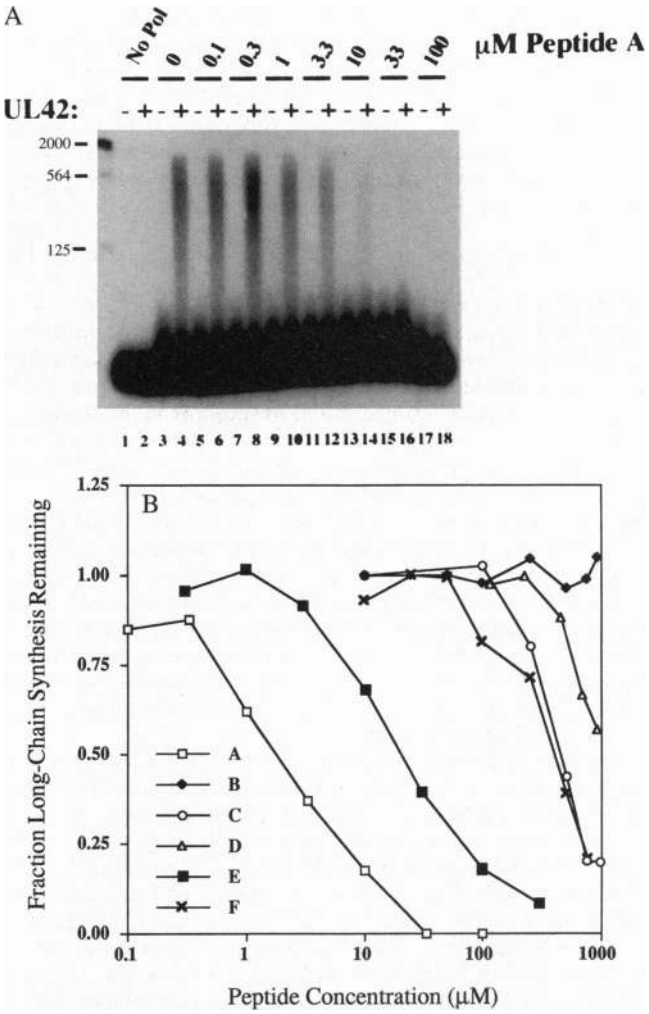

FIG. 4. (*A*) Inhibition of HSV DNA polymerase by peptide A. Polymerase assays using ^{32}P-labeled oligo(dT) primers on a poly(dA) template were carried out in the presence of the indicated concentration (μM) of peptide A. Pol was omitted from the reactions in lanes 1 and 2, and UL42 was added as indicated. Samples were electrophoresed in an alkaline 4% agarose gel. Positions of DNA size markers (bases) are indicated at left. The slight stimulation of long-chain synthesis at 0.3 μM peptide A was not reproducible. (*B*) Peptide dose–response curves. Long-chain DNA synthesis in the presence of various amounts of each peptide was quantified. Values are expressed as a fraction of the value obtained in the absence of peptide.

requires a stable interaction between the two subunits, as *pol* and *UL42* mutations that specifically impair the interaction prevented the increase in chain length in this assay (data not shown).

As hypothesized, peptide A inhibited long-chain synthesis (Fig. 4*A*, compare lanes 4 and 14, for example), but had little effect on the products synthesized by Pol alone (compare lanes 3 and 13). Importantly, in reaction mixtures containing UL42, only long-chain synthesis was inhibited, and at peptide concentrations below 100 μM, short-chain synthesis was unaffected (compare lanes 4 and 16). This is consistent with the proposed mechanism of the peptide specifically blocking the Pol–UL42 association.

An 18-Residue Peptide Corresponding to Helix II Specifically Inhibits Long-Chain DNA Synthesis. We then derived dose–response curves for the effects of each peptide on short-chain (data not shown) and long-chain (Fig. 4*B*) DNA synthesis, as a means of assessing the relative importance of the different regions of the C terminus of Pol. Peptide A was the most potent inhibitor of long-chain polymerization, with an

IC_{50} of 2 μM, and showed considerable specificity, as 25-fold more peptide was required to similarly inhibit DNA synthesis by Pol alone (Fig. 4*A*). Of the shorter peptides, peptide E from helix II (residues 1218–1235) was the most potent, inhibiting UL42-dependent long-chain DNA synthesis with an IC_{50} value of 30 μM (Fig. 4*B*). In contrast, its IC_{50} was >1500 μM for short-chain synthesis catalyzed by Pol alone (data not shown). Interestingly, peptide F, corresponding to most of helix II except for three N-terminal residues (Fig. 1), was markedly less potent than peptide E (Fig. 4*B*) but also had only about one-fifth its helical content (data not shown). Peptides B–D, corresponding to helix I and the loop region, and a variety of other peptides ranging from 18 to 30 residues in length were all much less potent than peptides A and E and showed little or no evidence of specificity for UL42-mediated long-chain synthesis compared with synthesis catalyzed by Pol alone (Fig. 4*B* and data not shown).

Specificity of Inhibition. The ratios of IC_{50} values for short- and long-chain synthesis of peptides A and E (25:1 and >50:1, respectively) and the lack of potency of other peptides argue that peptides A and E specifically inhibit processive DNA synthesis by the Pol–UL42 complex. As a further test of specificity, we examined the effects of these peptides on the analogous interaction between a cellular DNA polymerase, DNA polymerase δ, and its processivity factor, PCNA (21, 22). As expected, in the absence of PCNA, Pol δ synthesized short DNA products (Fig. 5, compare lanes 1 and 2). However, neither short-chain nor PCNA-dependent long-chain synthesis was inhibited by peptide E, at concentrations as high as 330 μM (Fig. 5). Similarly, peptide A at 100 μM showed no inhibition of Pol δ–PCNA DNA synthesis (data not shown). We conclude that peptides A and E are specific inhibitors of HSV Pol–UL42 long-chain DNA synthesis.

DISCUSSION

A Model for the Structure of the UL42 Binding Site of HSV Pol. CD spectroscopy of peptides A, B, and E in aqueous solution indicated that they contained substantial levels of α-helix, consistent with earlier predictions of the structure of the extreme C terminus of Pol (6). The degree of helicity of peptides B and E, corresponding to predicted helices I and II, respectively, depended on peptide concentration, suggesting that the peptides self-associated. This was not unexpected, given the predicted amphipathic nature of the helices (6) and the observation that short monomeric α-helices are generally

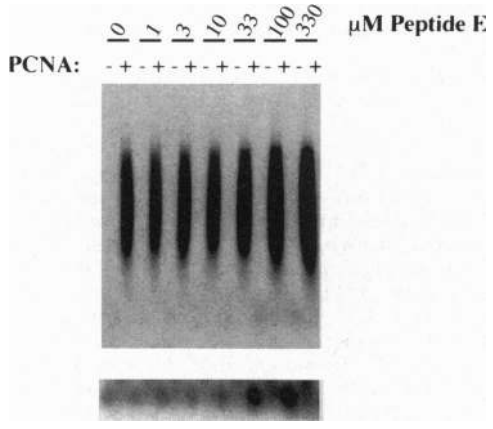

FIG. 5. Titration of peptide E with Pol δ and PCNA. Polymerase assays were carried out in the presence of the indicated concentrations of peptide, with PCNA included as shown. A longer exposure is shown of the bottom portion of the gel to allow visualization of the short DNA products synthesized by Pol δ in the absence of PCNA. Nonspecific stimulation of polymerase activity by high concentrations of noninhibitory peptides was also often seen with HSV Pol (data not shown).

unstable in aqueous solution (23). In contrast, the helicity of peptide A was apparently independent of peptide concentration, and equilibrium analytical centrifugation confirmed that the peptide was monomeric in solution. Interestingly, the helical content of peptide A was similar to that expected from the helical contents of peptides B and E at high concentrations.

One potential explanation for these findings is that the increased length of peptide A may permit the formation of a monomeric linear α-helix. We think this is unlikely because the helix would still be amphipathic and expected to self-associate, as did peptides B and E. Instead, we favor a structure for peptide A in which intramolecular interactions, possibly including helix–helix interactions, form a discrete hairpin-like structure, permitting stabilization of short stretches of α-helix. This model is supported by the monomeric nature of peptide A and the propensity of peptides corresponding to the predicted individual helices to form higher-order structures. Preliminary nuclear magnetic resonance spectroscopic investigations of peptide A are consistent with its helical content detected by CD and with intramolecular interactions (Q. X. Hua, P.D., C.E.D., D.M.C., and M. Weiss, unpublished results). Although we cannot exclude the possibility that the C-terminal 36 residues of Pol fold into a different conformation in the intact protein, it would be surprising if the α-helical character of the region were not preserved (24).

The observation that peptides A and E inhibited the functional consequences of the Pol–UL42 interaction is most simply interpreted by the direct involvement of the corresponding regions of Pol in UL42 binding. In confirmation of this, recent evidence from plasmon surface resonance studies indicates that peptide A can bind directly to UL42 (S. Mahdiyoun and D.M.C., unpublished results). Overall, this is consistent with mutational results that implicated the C-terminal 18–40 residues as critical for UL42 binding (6, 8, 9, 25), although the inhibitory effect of peptide E appears to argue against conclusions that residues downstream of aa 1216 are not important (9, 26). The 10-fold lower potency of peptide E relative to peptide A could be interpreted as indicating that UL42 makes substantial contact with residues between aa 1200 and 1218 (the N-terminal boundaries of peptides A and E, respectively). Alternatively, the helix II region may only be able to interact meaningfully with UL42 when in an appropriate conformation, either when stabilized intramolecularly (e.g., when within peptide A) or intermolecularly (e.g., by self-association of peptide E). These possibilities can be addressed experimentally; however, we note that the concentration of peptide E required for substantial helical content (≈20 μM; data not shown) is similar to that required for inhibition of long-chain synthesis (≈30 μM; Fig. 4*B*). Recent work measuring the relative affinities for UL42 of wild-type Pol and a mutant Pol lacking the C-terminal 27 residues led to the conclusion that the deleted region was required for 75% of the binding energy (25). Nevertheless, although the C terminus of Pol is most important for binding of UL42, upstream residues may still play a role.

A Class of DNA Polymerase Inhibitors That Act by Blocking Subunit Interactions. We have shown that peptides corresponding to the C terminus of HSV Pol can inhibit long-chain DNA synthesis mediated by Pol plus UL42 to a much greater extent than polymerization mediated by Pol alone. In addition, these peptides required much higher concentrations to inhibit synthesis by cellular DNA Pol δ. Thus, we conclude that peptides A and E are specific inhibitors of HSV DNA polymerase that act by blocking UL42-dependent long-chain synthesis. This would represent a class of polymerase inhibitors whose mechanisms differ from those of most known inhibitors, which act by binding to substrate- or product-binding sites. Our results are consistent with the peptides acting as hypothesized by blocking the protein–protein interaction between Pol and UL42. In support of this is the preliminary finding that peptide

A can bind directly to UL42 (S. Mahdiyoun and D.M.C., unpublished results) and the work of Marsden *et al.* (25), who recently found that a 27-residue peptide from the C terminus of Pol blocked UL42-stimulated Pol activity and directly inhibited UL42 binding to Pol.

In contrast, UL42-derived peptides were found generally to be nonspecific inhibitors of the Pol–UL42 complex (27). This difference may reflect the UL42-binding site on Pol being more conducive to peptide mimicry or may simply result from the choices of peptides. Extensive mutagenesis of UL42 has thus far failed to define a discrete region capable of binding Pol (7, 15, 26), raising the possibility that unlike Pol, the major interacting residues of UL42 may be noncontiguous.

Implications for Antiviral Drug Development. Genetic analyses of the Pol–UL42 interaction *in vitro* and in the context of the infected cell argue strongly that the interaction is essential for HSV replication and thus represents a valid drug target. Subunit interactions of HSV ribonucleotide reductase (28, 29) and interactions of the HSV VP16 transactivating protein with cellular proteins (30) have also been proposed as potential targets for therapeutic intervention. However, unlike the Pol–UL42 interaction, ribonucleotide reductase and VP16 transactivation are dispensable under certain circumstances (31, 32). Our results point to two routes to the rational design of drugs against the Pol–UL42 interaction. The first route stems from the biophysical data that indicate that the UL42-binding site of Pol folds into a discrete structure. Preliminary results suggest that a high-resolution structure of peptide A might be tractable by nuclear magnetic resonance spectroscopy (Q. X. Hua, P.D., C.E.D., D.M.C., and M. Weiss, unpublished results). With such a structure in hand, computer-aided design of small molecules that bind specifically and inhibit the Pol–UL42 interaction may be possible. Similar design efforts have recently abetted the discovery of inhibitors of other antiviral drug targets (e.g., refs. 33 and 34).

The second route to rational drug design stems from our identification of peptides that specifically inhibit long-chain DNA synthesis by HSV DNA polymerase. This suggests that these peptides, or preferably shorter derivatives thereof, could form the basis for the synthesis of peptidomimetics that could inhibit HSV replication. Encouragement for this approach has come from the synthesis of a drug based on a peptide corresponding to the subunit interface of the HSV ribonucleotide reductase. This drug is >10,000-fold more potent for inhibition of ribonucleotide reductase than the starting peptide and is capable of exerting antiviral effects under conditions where the reductase is required for HSV replication (38).

It is our hope that one or both of these routes will lead to the discovery of clinically useful anti-HSV drugs and will suggest similar strategies for inhibiting other dimeric herpesvirus DNA polymerases (35–37).

We thank J. Chafouleas, R. Déziel, M. Cordingley, and their colleagues of Bio-Méga/Boehringer Ingelheim for supplying peptides and communicating unpublished results; D. Wiley and S. Harrison for the use of their CD spectropolarimeter; B. Stillman for supplying Pol δ and PCNA; K. Weisshart for purifying HSV Pol and UL42; H. Marsden for communicating results prior to publication; M. Weiss for helpful discussions; J. Brown for help in manuscript preparation; and I. Brierley, C. Chow, and B. Horsburgh for constructive criticisms. This work was supported by National Institutes of Health Grants AI26077 and AI19838 to D.M.C.

1. Coen, D. M. (1992) *Semin. Virol.* **3,** 3–12.
2. Hirsch, M. S. & Schooley, R. T. (1989) *N. Engl. J. Med.* **320,** 313–314.
3. Kost, R. G., Hill, E. L., Tigges, M. & Straus, S. E. (1993) *N. Engl. J. Med.* **329,** 1777–1782.
4. Gottlieb, J., Marcy, A. I., Coen, D. M. & Challberg, M. D. (1990) *J. Virol.* **64,** 5976–5987.
5. Hernandez, T. R. & Lehman, I. R. (1990) *J. Biol. Chem.* **265,** 11227–11232.
6. Digard, P., Bebrin, W., Weisshart, K. & Coen, D. M. (1993) *J. Virol.* **67,** 398–406.
7. Digard, P., Chow, C., Pirrit, L. & Coen, D. M. (1993) *J. Virol.* **67,** 1159–1168.
8. Stow, N. (1993) *Nucleic Acids Res.* **21,** 87–92.
9. Tenney, D. J., Micheletti, P. A., Stevens, J. T., Hamatake, R. K., Matthews, J. T., Sanchez, A. R., Hurlburt, W. W., Bifano, M. & Cordingley, M. G. (1993) *J. Virol.* **67,** 543–547.
10. Cantor, C. R. & Schimmel, P. R. (1980) *Biophysical Chemistry, Part 2: Techniques for the Study of Biological Structure and Function* (Freeman, San Francisco), pp. 623–631.
11. Edelstein, S. J. & Schachman, H. K. (1973) *Methods Enzymol.* **27,** 83–97.
12. Eisenstein, E., Osborne, J. C., Jr., Chaiken, I. M. & Hensley, P. (1984) *J. Biol. Chem.* **259,** 5139–5145.
13. Johnson, M. L. & Faunt, L. M. (1992) *Methods Enzymol.* **210,** 1–37.
14. Brooks, I., Watts, D. G., Soneson, K. K. & Hensley, P. (1994) *Methods Enzymol.* **240,** 459–478.
15. Tenney, D. J., Hurlburt, W. W., Bifano, M., Stevens, J. T., Micheletti, P. A., Hamatake, R. K. & Cordingley, M. G. (1993) *J. Virol.* **67,** 1959–1966.
16. Hamatake, R. K., Bifano, M., Tenney, D. J., Hurlburt, W. W. & Cordingley, M. G. (1993) *J. Gen. Virol.* **74,** 2181–2189.
17. Digard, P. & Coen, D. M. (1990) *J. Biol. Chem.* **265,** 17393–17396.
18. Gibbs, J. S., Chiou, H. C., Hall, J. D., Mount, D. W., Retondo, M. J., Weller, S. K. & Coen, D. M. (1985) *Proc. Natl. Acad. Sci. USA* **82,** 7969–7973.
19. Johnson, W. C. (1990) *Proteins Struct. Funct. Genet.* **7,** 205–214.
20. Chen, Y.-H., Yang, J. T. & Chau, K. H. (1974) *Biochemistry* **13,** 3350–3358.
21. Bravo, R., Frank, R., Blundell, P. A. & MacDonald-Bravo, H. (1987) *Nature (London)* **326,** 515–517.
22. Prelich, G., Tan, C. K., Kostura, M., Mathews, M. B., So, A. G., Downey, K. M. & Stillman, B. (1987) *Nature (London)* **326,** 517–520.
23. Scholtz, J. M. & Baldwin, R. L. (1992) *Annu. Rev. Biophys. Biomol. Struct.* **21,** 95–118.
24. Dyson, H. J., Merutka, G., Waltho, J. P., Lerner, R. A. & Wright, P. E. (1992) *J. Mol. Biol.* **226,** 795–817.
25. Marsden, H., Murphy, M., McVey, G., MacEachran, K., Owsianka, A. & Stow, N. (1994) *J. Gen. Virol.* **75,** 3127–3135.
26. Monahan, S. J., Barlam, T. F., Crumpacker, C. S. & Parris, D. S. (1993) *J. Virol.* **67,** 5922–5931.
27. Owsianka, A., Hart, G., Murphy, M., Gottlieb, J., Boehme, R., Challberg, M. & Marsden, H. S. (1993) *J. Virol.* **67,** 258–264.
28. Cohen, E. A., Gaudreau, P., Brazeau, P. & Langelier, Y. (1986) *Nature (London)* **321,** 441–443.
29. Dutia, B. M., Frame, M. C., Subak-Sharpe, J. H., Clark, W. N. & Marsden, H. S. (1986) *Nature (London)* **321,** 439–441.
30. Haigh, A., Greaves, R. & O'Hare, P. (1990) *Nature (London)* **344,** 257–259.
31. Goldstein, D. J. & Weller, S. K. (1988) *J. Virol.* **62,** 196–205.
32. Ace, C. I., McKee, T. A., Ryan, J. M., Cameron, J. M. & Preston, C. M. (1989) *J. Virol.* **63,** 2260–2269.
33. Lam, P. Y.-S., Jadhav, P. K., Eyermann, C. J., Hodge, C. N., Ru, Y., Bacheler, L. T., Meek, J. L., Otto, M. J., Rayner, M. M., Wong, Y. N., Chang, C.-H., Weber, P. C., Jackson, D. A., Sharpe, T. R. & Erickson-Viitanene, S. (1994) *Science* **263,** 380–384.
34. von Itzstein, M., Wu, W.-Y., Kok, G. B., Pegg, M. S., Dyason, J. C., Jin, B., Phan, T. V., Smythe, M. L., White, H. F., Oliver, S. W., Colman, P. M., Varghese, J. N., Ryan, D. M., Woods, J. M., Bethell, R. C., Hotham, V. J., Cameron, J. M. & Penn, C. R. (1993) *Nature (London)* **363,** 418–423.
35. Agulnick, A. D., Thompson, J. R., Iyengar, S., Pearson, G., Ablashi, D. & Ricciardi, R. P. (1993) *J. Gen. Virol.* **74,** 1003–1009.
36. Ertl, P. F. & Powell, K. L. (1992) *J. Virol.* **66,** 4126–4133.
37. Li, J.-S., Zhou, B.-S., Dutschman, G. E., Grill, S. P., Tan, R.-S. & Cheng, Y.-C. (1987) *J. Virol.* **61,** 2947–2949.
38. Liuzzi, M., Déziel, R., Moss, N., Beaulieu, P., Bonneau, A.-M., Bousquet, C., Chafouleas, J. G., Garneau, M., Jaramillo, J., Krogsrud, R. L., Lagacé, L., McCollum, R. S., Nawoot, S. & Guindon, Y. (1994) *Nature (London)* **372,** 695–698.